PAPER

Check for updates

Impact of ether coordination on the solid-state luminescence of a lithium β-diketiminate complex†

Shunichiro Ito, [ID] [a,b] Kazuo Tanaka [ID] *[a,b] and Yoshiki Chujo[a]
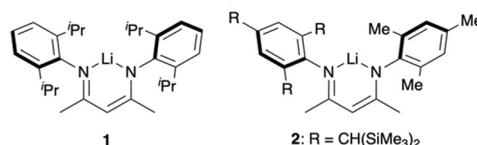
A solid-state luminescent lithium β-diketiminate complex was synthesized by the reaction of the corresponding proligand and *n*-butyllithium in hexane. The complex showed a low-coordinated structure in the solution and crystalline states. On the other hand, the lithium complex reacted with diethyl ether, tetrahydrofuran, and 1,4-dioxane to form three-coordinated complexes, which showed lower emission efficiency. Remarkably, the photoluminescence of the crystal of the low-coordinate species was quenched by the treatment with the diethyl ether vapor. NMR spectroscopy and X-ray diffraction analyses revealed that diethyl ether reacts with the complex to afford the three-coordinated ether adduct even in the crystalline state. To the best of our knowledge, this is the first report on the luminescence switching in crystalline materials based on the modification of the coordination number on a lithium atom.
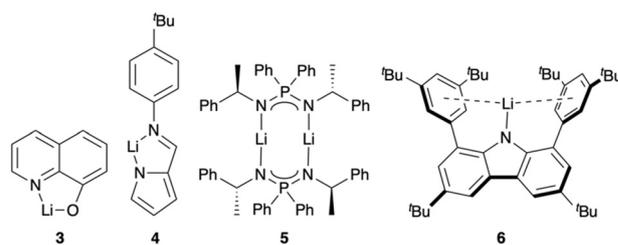
Introduction

Inorganic and organometallic alkali metal compounds are intermediates of a tremendous variety of organic and organometallic compounds because of their high reactivity. The coordination environment around metals is well known to be a key factor in controlling the reactivity of compounds and the selectivity of reactions.[1–13] The most common coordination number of alkali metals is four. Nevertheless, over the past two decades, the isolation of two-coordinated or donor-free alkali metal complexes has been accomplished because of the development of sterically encumbered ligands.[5,14–22] This class of complexes exhibits strong Lewis acidity originating from their coordinative unsaturation. β-Diketiminate ligands are one of the important scaffolds for isolating base-free alkali metal complexes, such as **1**[15] and **2** (Chart 1, top).[16] The sterically hindered substituents on the nitrogen atoms are essential for preventing the strong interactions with Lewis bases. In addition to studies on their structures, recent studies have also focused on their catalytic activities[23] and luminescent properties.[24–28] In particular, lithium quinolinolate **3** has been studied as an emitting and electron-transporting layer in organic light-emitting diodes.[24] More recently, the lithium

complexes of pyrrolide **4**,[25] iminophosphonamide **5**,[26] and carbazolide **6**[27] have been developed, exhibiting fruitful properties (Chart 1, middle), for instance, efficient luminescence, thermally activated delayed fluorescence, and solid-state luminescence. Importantly, it was suggested that the base-free
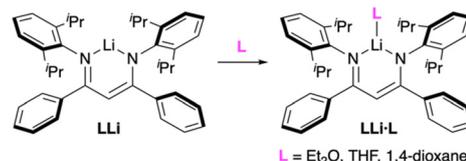

Chart 1 Chemical structures of selected lithium complexes and molecules investigated in this work.

aDepartment of Polymer Chemistry, Graduate School of Engineering, Kyoto University, Katsura, Nishikyo-ku, Kyoto 615-8510, Japan
bDepartment of Technology and Ecology, Graduate School of Global Environmental Studies, Kyoto University, Katsura, Nishikyo-ku, Kyoto 615-8510, Japan

complex of **6** emits more efficiently than the corresponding toluene adduct in the solid states.[27] Meanwhile, as the difference in the photoluminescence quantum yield (up to 1.7 times) was still limited, there is much room for exploring the impact of base coordination on the photophysical properties of lithium complexes.

In this context, π-extended β-diketimine ligands are intriguing candidates for constructing luminescent lithium complexes because their group 13 metal complexes exhibit aggregation-induced emission (AIE) and crystallization-induced emission (CIE) properties.[29–39] These solid-state luminescent properties and environment sensitiveness are advantageous for constructing film-type optical sensors and detection devices for tiny environmental changes and weak external stimuli. Therefore, we envisioned that stimuli-responsive materials might be obtained based on the strong Lewis acidity of base-free lithium complexes with sterically encumbered β-diketiminates. Herein, we report the preparation and characterization of a luminescent base-free lithium β-diketimine complex and the switching of solid-state luminescence properties by coordination with various ethers (Chart 1, bottom). The base-free complex exhibited efficient luminescence in the crystalline state, while the ether adducts showed lower emission efficiencies. Interestingly, the photoluminescence in the crystalline state was dramatically quenched by the vapor fuming with diethyl ether. From the results of single-crystal X-ray diffraction analyses, it was found that diethyl ether coordinates to the lithium atom to give the three-coordinated species even in the crystalline state.

Results and discussion

The base-free lithium β-diketimine complex (**LLi**) was synthesized by the reaction of *n*-butyllithium with the bulky and π-conjugated β-diketimine proligand (**LH**) in hexane at room temperature or under moderate heating up to *ca.* 30 °C (Scheme 1). The use of non-coordinating solvents, like hexane, is essential to obtain base-free alkali metal complexes.[5,14–22] Although the initial yellow suspension of the proligand was not emissive, the suspension of the reaction mixture exhibited strong green emission after the reaction proceeded. The single crystals containing **LLi** suitable for X-ray analysis were obtained from the toluene/hexane (1/1, v/v) mixed solvent solution at 10 °C. Furthermore, it was found that **LLi** reacts with various ethers, involving diethyl ether (Et$_2$O), tetrahydrofuran (THF), and 1,4-dioxane (DOX), in the recrystallization process

from ethers/hexane (1/1, v/v) to form the corresponding three-coordinated ether adducts **LLi·OEt$_2$**,[40] **LLi·THF**, and **LLi·DOX**. The chemical structures of the complexes in solutions were confirmed by ^{1}H and ^{13}C{^{1}H} NMR spectroscopy in C$_6$D$_6$ and single-crystal X-ray diffraction analysis. All lithium complexes in this study are highly sensitive to water and air. Therefore, all measurements were carried out under nitrogen or argon atmosphere. When the complexes were exposed to either water or air, they rapidly decompose into **LH**, while no other decomposed product was detectable.

LLi, **LLi·OEt$_2$**, **LLi·THF**, and **LLi·DOX** formed crystals belonging to the monoclinic $P2_1/n$, triclinic $P\bar{1}$, triclinic $P\bar{1}$, and tetragonal $P42/n$ space groups, respectively (Table S1†). The crystallographic parameters of **LLi·OEt$_2$** agreed with the reported data.[40] In all crystals, each asymmetric unit included a single crystallographically independent complex molecule. Only for the case of **LLi·DOX**, its asymmetric unit involved an additional free DOX molecule. The ^{1}H NMR spectrum of **LLi·DOX** after drying *in vacuo* showed a 1:1 molar ratio of the complex and DOX, indicating that the free DOX molecules in the crystal can be removed. The crystal structures of the complexes are shown in Fig. 1, and the selected structural parameters are listed in Table 1. Notably, in the crystalline state of **LLi**, the lithium cation was not coordinated to any solvent molecules and instead interacted with the carbon atoms of the phenyl ring in a neighboring molecule with the formation of the polymeric packing structure (Li···C7 = 2.670(4), Li···C8 = 2.572(4) Å). These Li···C interactions are weaker than the reported data in [Li(Dipp)NCH$_2$CH$_2$N(Dipp)Li]$_2$ (2.153(10) Å)[41] and stronger than those in the related β-diketimine complex, Dipp$_2$nacnacLi (2.834(7) Å).[15] The six-membered LiN$_2$C$_3$ ring of the complexes was nearly planar with the slight deviation of one of the nitrogen atoms from the least-squares plane of the other five atoms (**LLi**, 0.2657(26) Å; **LLi·OEt$_2$**, 0.1550(34) Å; **LLi·THF**, 0.1296(26) Å; **LLi·DOX**, 0.1004(32) Å). In addition, no apparent bond alteration was observed within the N$_2$C$_3$ moiety, indicating the delocalization of π-electrons. Interestingly, the average Li–N bond length increased from 1.901(3) and 1.881(3) Å for **LLi** to 1.919(4) and 1.929(4) Å for **LLi·OEt$_2$**, 1.903(3) and 1.910(3) Å for **LLi·THF**, and 1.902(4) and 1.918(4) Å for **LLi·DOX**. This result suggests that the coordination of diethyl ether weakens the Li–N bonds. This weakening effect results in a more acute coordination angle for the ether adducts (98.4(2)°) than for **LLi** (99.4(1)°), **LLi·THF** (98.8(1)°), and **LLi·DOX** (98.5(2)°).

Photophysical properties of the synthesized complexes were evaluated with UV–vis absorption and photoluminescence (PL)
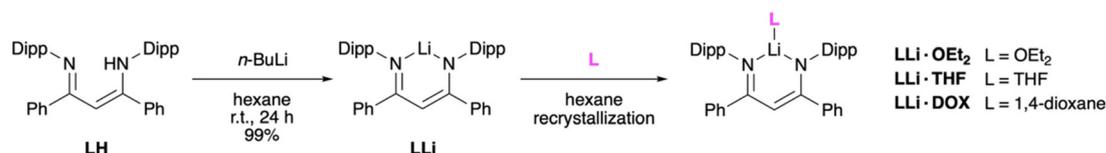
Scheme 1 Synthetic scheme of the base-free lithium complex **LLi** and the ether adduct **LLi·OEt$_2$** (Dipp = 2,6-diisopropylphenyl).
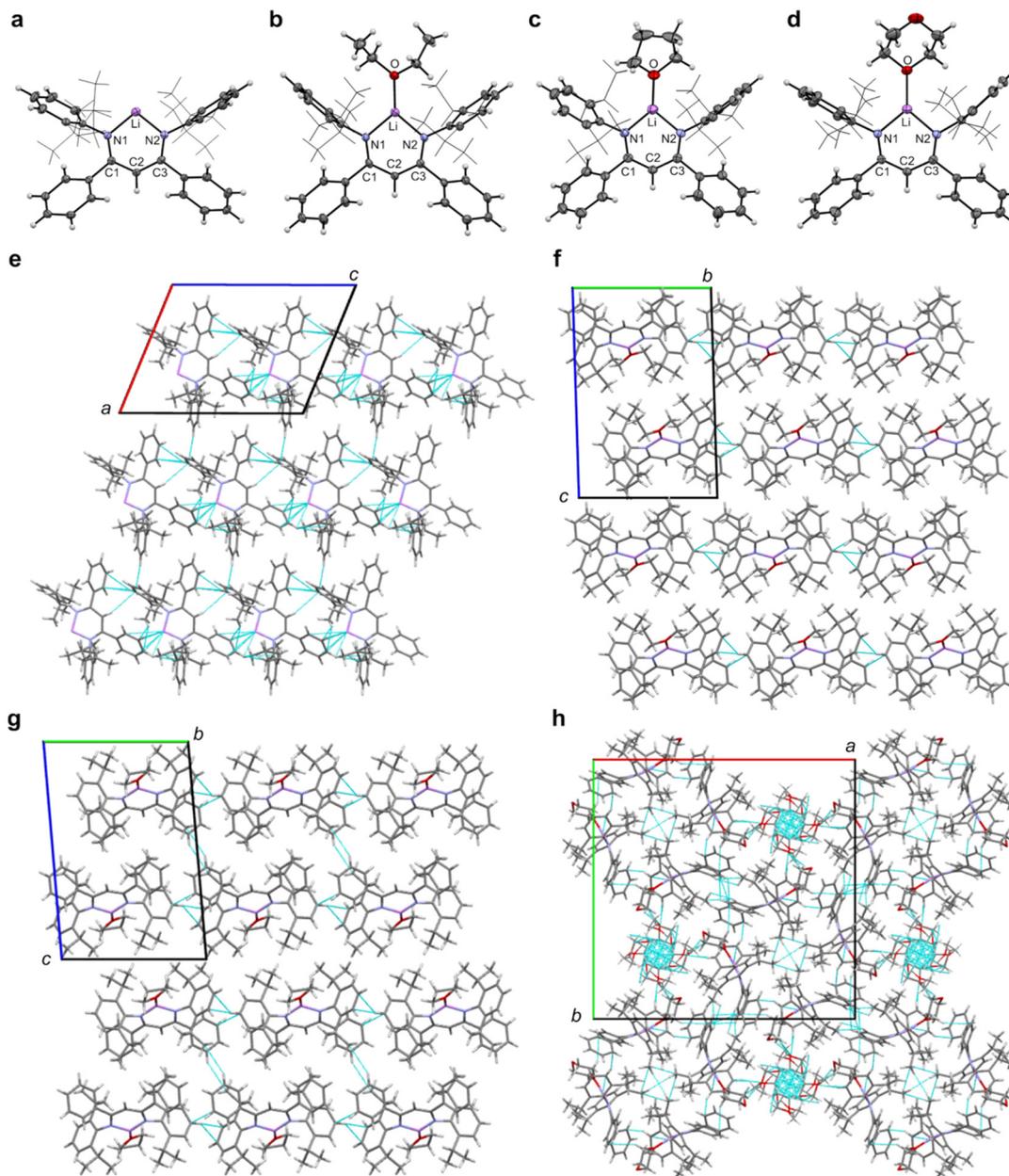
Fig. 1 Single-crystal structures of (a) **LLi**, (b) **LLi·OEt$_2$**, (c) **LLi·THF**, and (d) **LLi·DOX** (50% displacement ellipsoids). Only the crystal of **LLi·DOX** was obtained as a 1 : 1 solvated crystal with 1,4-dioxane. Isopropyl groups, and the free 1,4-dioxlane molecule in a solvent channel are shown in wire-frame style and omitted, respectively, for clarity. Packing structures of (e) **LLi**, (f) **LLi·OEt$_2$**, (g) **LLi·THF**, and (h) **LLi·DOX**. Dashed cyan lines show short contacts (<sum of van der Waals radii). Atom legends: gray, carbon; white, hydrogen; blue, nitrogen; purple, lithium; red, oxygen.

measurements (Fig. 2a–d and Table 2). All measurements were carried out under a N$_2$ atmosphere because of the instability of the complexes under aerobic conditions. All complexes showed similar absorption spectra peaked at around 365 nm. Additionally, emission from their dilute solution (2-methylpentane (2MP)/toluene = 99/1, 1 × 10^{-5} M) was not detectable at room temperature and even in the frozen solution at 77 K. The absolute luminescence quantum yields were not determined due to small values below the detection limit (<0.01). On the other hand, intense green PL was observed from crystalline **LLi** even at room temperature (Φ_{PL} = 0.65, Fig. 2e). This result clearly indicates that **LLi** possesses the CIE property, similarly to the related β-diketiminate complexes containing the group 13 elements.[29–39] The molecular motions in the excited states, like intramolecular vibrations[34] and structural deformations,[37] could open the channel for the nonradiative decay of the excited molecules in solution states, while the rigid crystalline packing could annihilate such nonradiative decay processes. Remarkably, in contrast to the base-free complex, the ether adducts exhibited only slight enhancement

Table 1 Selected structural parameters of **LLi**, **LLi·OEt₂**, **LLi·THF**, and **LLi·DOX**

LLi		LLi·OEt₂		LLi·THF		LLi·DOX	
Bond							
	$d/\text{Å}$		$d/\text{Å}$		$d/\text{Å}$		$d/\text{Å}$
Li–N1	1.901(3)	Li–N1	1.919(4)	Li–N1	1.903(3)	Li–N1	1.902(4)
Li–N2	1.881(3)	Li–N2	1.929(4)	Li–N2	1.910(3)	Li–N2	1.918(4)
N1–C1	1.329(3)	N1–C1	1.329(3)	N1–C1	1.326(2)	N1–C1	1.324(2)
N2–C3	1.321(3)	N2–C3	1.330(3)	N2–C3	1.326(2)	N2–C3	1.324(2)
C1–C2	1.411(2)	C1–C2	1.413(3)	C1–C2	1.409(2)	C1–C2	1.411(3)
C2–C3	1.413(2)	C2–C3	1.419(3)	C2–C3	1.415(2)	C2–C3	1.415(3)
		O–Li	1.929(5)	O–Li	1.899(4)	O–Li	1.918(4)
Angle							
	$\theta/°$		$\theta/°$		$\theta/°$		$\theta/°$
N1–Li–N2	99.4(1)	N1–Li–N2	98.4(2)	N1–Li–N2	98.8(1)	N1–Li–N2	98.5(2)
		O–Li–N1	129.7(2)	O–Li–N1	132.1(2)	O–Li–N1	128.8(2)
		O–Li–N2	129.8(2)	O–Li–N2	127.1(2)	O–Li–N2	130.7(2)
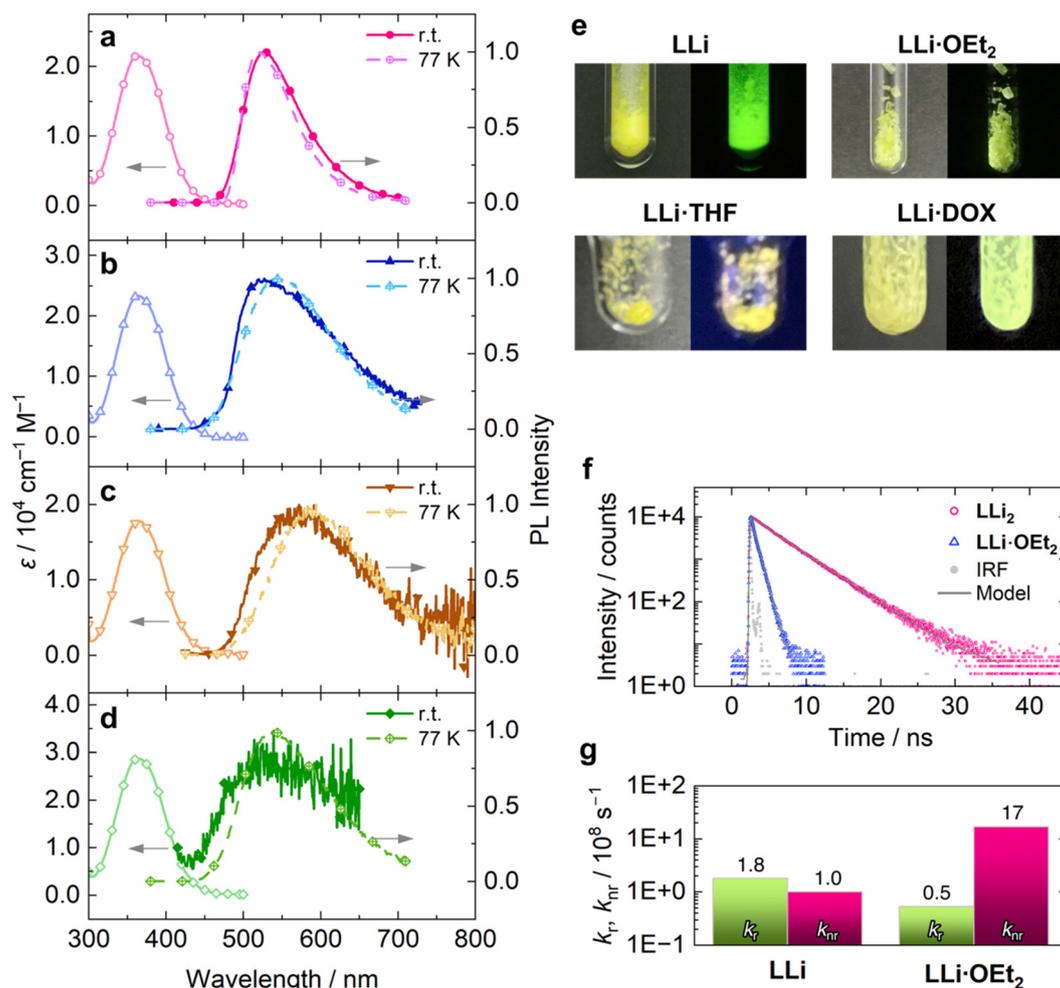
Fig. 2 UV–vis absorption spectra in dilute 2MP/toluene (99/1) solutions (1 × 10⁻⁵ M) and PL spectra of crystals of (a) **LLi**, (b) **LLi·OEt₂**, (c) **LLi·THF**, and (d) **LLi·DOX**. (e) Pictures of crystals of the complexes under room light (left panels) and UV irradiation (right panels). (f) PL decay profiles of the crystals of **LLi** (magenta open circles) and **LLi·OEt₂** (blue open squares) upon excitation at 375 nm with an LED laser. Gray solid lines are the fitted curves. Instrument response function (IRF) is also shown (gray closed circles). (g) Calculated radiative (k_r) and non-radiative (k_{nr}) decay rate constants of the complexes.

Table 2 Photophysical properties of the complexes[a]

| | Temperature | Solution[b] | Crystal | |
		λ_{abs}/nm	λ_{PL}/nm	$\Phi_{PL}{}^d$
LLi	r.t.	364	527	0.65
	77 K	—[c]	521	0.90
LLi·OEt₂	r.t.	363	527	0.03
	77 K	—[c]	543	0.14
LLi·THF	r.t.	366	572	0.03
	77K	—[c]	594	0.06
LLi·DOX	r.t.	364	539	0.08
	77K	—[c]	535	0.32

[a] PL spectra and absolute quantum yields were recorded with the photoexcitation at 360 nm. [b] 2MP/toluene (99/1, v/v) solution (1×10^{-5} M). [c] Not determined. [d] Absolute PL quantum yield determined with the integration sphere method.

of the emission by crystallization ($\Phi_{PL} = 0.03$ for **LLi·OEt₂**, 0.03 for **LLi·THF**, and 0.08 for **LLi·DOX**, Fig. 2e).

In order to gain further insights into the photophysical processes of the complexes, luminescence lifetimes of the crystals of **LLi** and **LLi·OEt₂** were measured by the time-correlated single photon counting (TCSPC) measurement (Fig. 2f and Table 3). The nanosecond-order lifetimes strongly suggested that the luminescence from both crystals should be assigned to fluorescence. As shown in Table 3, the emission decay of **LLi** includes the relatively long components (1.71 and 3.81 ns), whereas the luminescence from **LLi·OEt₂** decays with the sub-nanosecond lifetimes (0.26 and 0.65 ns). The nonradiative decay rate constant (k_{nr}) of **LLi·OEt₂** was 17 times larger than that of **LLi**, while the radiative decay rate constant (k_r) of the ether adduct was less than one-third of that of the base-free complex (Fig. 2g and Table 3). These results indicate that significantly fast nonradiative decay processes hamper the efficient luminescence of **LLi·OEt₂**, and such processes are absent in the crystals of **LLi**. The molecular motions of the coordinated ether molecules could be responsible for such quenching paths.

To investigate the electronic nature of the complexes, density functional theory (DFT) calculations were carried out. Geometries of the compounds were optimized at the CAM-B3LYP/6-31G(d,p) level of theory. The optimized structures were confirmed as local minima by performing frequency calculations at the same level. The calculated energy diagrams and the Kohn–Sham (KS) frontier orbital distributions of the complexes are shown in Fig. 3. The energies of the KS highest occupied molecular orbitals (HOMOs) were hardly affected by

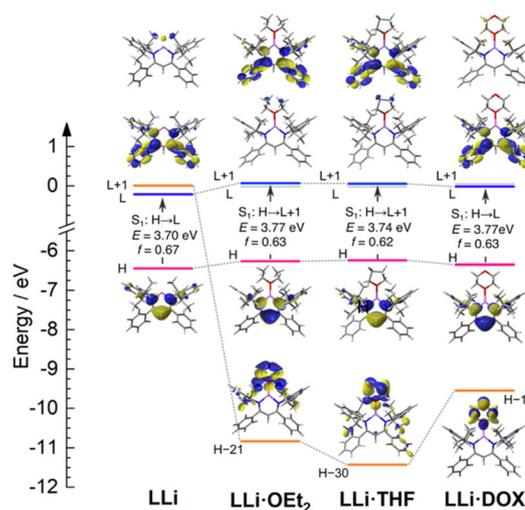**Fig. 3** Calculated Kohn–Sham (KS) orbital energy diagram, transition energy (E), and oscillator strength (f). KS frontier orbital distributions are shown (isovalue = 0.03). H and L denote the HOMO and LUMO, respectively.

the ether. The KS lowest unoccupied molecular orbital (LUMO) of **LLi**, the next LUMO (LUMO+1) of **LLi·OEt₂** and **LLi·THF**, and the LUMO of **LLi·DOX** assigned to the LUMO of the N_2C_3 moiety were located in almost the same energy region. On the other hand, the LUMO+1 of **LLi**, which was composed mainly of the vacant 2p orbital of the lithium atom, was significantly stabilized by the complexation owing to the bonding interaction between the vacant orbital and the lone pair of ether. Additionally, the LUMO of **LLi·OEt₂** and **LLi·THF** and LUMO+1 of **LLi·DOX**, which were assigned to the antibonding orbital in the ether moiety, seemed to be degenerated with the LUMO+1 because there is almost no interaction between the π* orbital of the ligand and the σ* orbital of the ether.

The S_0–S_1 electronic transitions were calculated with time-dependent DFT (TD-DFT) at the CAM-B3LYP/6-311++G(d,p) level of theory and the results are shown in Fig. 3 and Table 4. The S_1 states of all complexes possessed the same character of the π–π* transition mainly located at the N_2C_3 moiety. Consequently, the transition energy was not disturbed independently of whether the lithium atom was coordinated by the ethers or not. These results are consistent with the experimental observation of the UV–vis absorption spectra in which the complexes exhibit almost identical absorption bands. It is assumed that an increase in the degree of molecular motions

Table 3 Luminescence lifetimes and decay rate constants of the complexes at crystalline states[a]

	τ_1/ns ($f_1{}^b$)	τ_2/ns ($f_2{}^b$)	χ^2	$\langle\tau\rangle^c$/ns	$k_r{}^d/10^8$ s⁻¹	$k_{nr}{}^d/10^8$ s⁻¹
LLi	1.71 (8.26%)	3.81 (91.74%)	1.17	3.63	1.8	1.0
LLi·OEt₂	0.26 (20.70%)	0.65 (79.30%)	1.22	0.57	0.5	17

[a] Excited at 375 nm with an LED laser. Decay curves were fitted with the multi-component exponential function: $I(t) = \sum_i [\alpha_i \exp(-\tau_i/t)]$. [b] Fraction of component i: $f_i = \alpha_i \tau_i / \sum_i \alpha_i \tau_i$. [c] Average lifetime: $\langle\tau\rangle = \left[\sum_i \alpha_i \tau_i^2\right] / \left[\sum_i \alpha_i \tau_i\right] = \sum_i f_i \tau_i$. [d] $k_r = \Phi_{PL}/\langle\tau\rangle$, $k_r = (1 - \Phi_{PL})/\langle\tau\rangle$.

Table 4 Results of TD-DFT calculations for the S_1 state of the complexes[a]

|	Energy[b]/eV	λ/nm	f[c]	Composition	Coefficient[d]
LLi	3.70	336	0.6707	HOMO → LUMO	0.68589
LLi·OEt₂	3.77	329	0.6281	HOMO → LUMO+1	0.67493
LLi·THF	3.74	332	0.6171	HOMO → LUMO+1	0.67896
LLi·DOX	3.77	329	0.6266	HOMO → LUMO	0.68099

[a] Calculated at the TD-CAM-B3LYP/6-311++G(d,p) level of theory. [b] Excitation energies between S_0 and S_1 states. [c] Oscillator strength. [d] Configuration interaction coefficient of the component for the S_0–S_1 transition.

might cause the luminescence quenching in the ether adducts. Indeed, the crystal structures of the complexes imply that the Li–N coordination could be weakened by the ether coordination. On the other hand, TD-DFT calculations for the monomeric and dimeric structures in the **LLi** crystal suggested that the relatively weak Li·π interactions in the crystal should not significantly affect the electronic transition properties (Table S12 and Fig. S1†).

To test whether the luminescence of the crystals of **LLi** was switched to that of **LLi·OEt₂** even in the solid state, the crystal-line powder of **LLi** was exposed to the vapor of diethyl ether in a glovebox. In a 50 mL sealed vial containing 3 mL of diethyl ether, a 5 mL open vial equipped with the crystalline powder of **LLi** was placed and subsequently stored at room temperature for 12 h. After the treatment, we confirmed that the emission from the crystals was critically weakened. The PL spectrum and the absolute PL quantum yield of the treated sample (0.02) were almost identical to those of the crystals of **LLi·OEt₂** (Fig. 4a). Powder X-ray diffraction (PXRD) patterns for the samples before and after treatment were identical with the simulated patterns of **LLi** and **LLi·OEt₂**, respectively, indicating that a crystal–crystal transition occurred by the ether vapor treatment (Fig. 4b). The ¹H NMR spectrum (Chart S5†) of the treated crystal after drying under vacuum showed the same peaks as those of **LLi·OEt₂**, and there was no residual signal assigned to **LLi**, indicating that the complexation between **LLi** and Et₂O is not reversed on simple vacuum drying. It can be said that the base-free lithium complex could be able to be utilized not only for the detection of Lewis bases but also for constructing other types of stimuli-responsive materials.
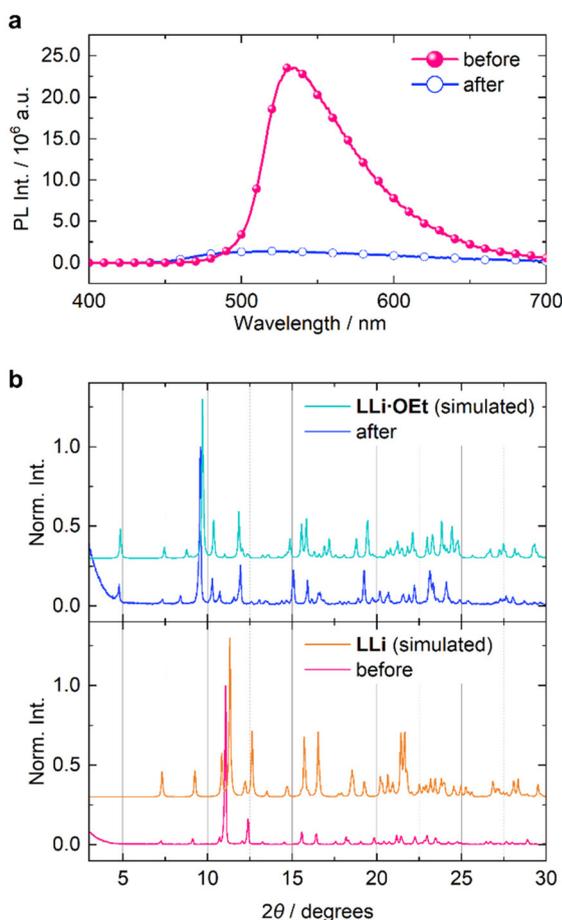
Fig. 4 (a) PL spectra before (magenta) and after (blue) the exposure of the diethyl ether vapor. (b) PXRD profiles before (magenta) and after (blue) Et₂O vapor treatment. Diffraction profiles simulated from SCXRD measurements are also shown.

Conclusion

The essentially two-coordinated lithium β-diketiminate complex **LLi** was synthesized by the reaction of *n*-butyllithium and the corresponding ligand in hexane. The complex exhibited strong green emission in the crystalline state, whereas its solution showed no PL. This is the first example of a CIE-active lithium complex. Single-crystal X-ray diffraction analysis revealed that the lithium atom of **LLi** moderately interacts with the C-bounded phenyl rings of the β-diketiminate ligand of a neighboring molecule. On the other hand, the ether adducts **LLi·OEt₂**, **LLi·THF**, and **LLi·DOX** exhibited only weak emission even in the crystalline state. Furthermore, it was demonstrated that the luminescence of the crystal of **LLi** was annihilated by fuming diethyl ether vapor through the formation of **LLi·OEt₂**. These results sheds new light on the development of stimuli-responsive materials based on the high Lewis acidity of base-free alkali metal complexes.

Data availability

The data supporting this article have been included as part of the ESI.†

Conflicts of interest

The authors declare no conflict of interest.

Acknowledgements

References

1 D. Seebach, *Angew. Chem., Int. Ed. Engl.*, 1988, **27**, 1624–1654.

2 H. J. Reich and D. P. Green, *J. Am. Chem. Soc.*, 1989, **111**, 8729–8731.

3 R. Neufeld, M. John and D. Stalke, *Angew. Chem., Int. Ed.*, 2015, **54**, 6994–6998.

4 U. Wietelmann and J. Klett, *Z. Anorg. Allg. Chem.*, 2018, **644**, 194–204.

5 A. I. McKay and M. L. Cole, *Dalton Trans.*, 2019, **48**, 2948–2952.

6 G. Fraenkel, A. Chow and W. R. Winchester, *J. Am. Chem. Soc.*, 1990, **112**, 6190–6198.

7 D. B. Collum, *Acc. Chem. Res.*, 1992, **25**, 448–454.

8 D. B. Collum, *Acc. Chem. Res.*, 1993, **26**, 227–234.

9 E. Weiss, *Angew. Chem., Int. Ed. Engl.*, 1993, **32**, 1501–1523.

10 B. L. Lucht and D. B. Collum, *Acc. Chem. Res.*, 1999, **32**, 1035–1042.

11 D. T. Carey, E. K. Cope-Eatough, E. Vilaplana-Mafé, F. S. Mair, R. G. Pritchard, J. E. Warren and R. J. Woods, *Dalton Trans.*, 2003, 1083–1093.

12 C. Strohmann and V. H. Gessner, *Angew. Chem., Int. Ed.*, 2007, **46**, 4566–4569.

13 R. E. Mulvey and S. D. Robertson, *Angew. Chem., Int. Ed.*, 2013, **52**, 11470–11487.

14 W. Clegg, E. K. Cope, A. J. Edwards and F. S. Mair, *Inorg. Chem.*, 1998, **37**, 2317–2319.

15 M. Stender, R. J. Wright, B. E. Eichler, J. Prust, M. M. Olmstead, H. W. Roesky and P. P. Power, *J. Chem. Soc., Dalton Trans.*, 2001, 3465–3469.

16 N. Takeda, H. Hamaki and N. Tokitoh, *Chem. Lett.*, 2004, **33**, 134–135.

17 H. Lee and M. Niemeyer, *Inorg. Chem.*, 2006, **45**, 6126–6128.

18 H. Hamaki, N. Takeda, T. Yamasaki, T. Sasamori and N. Tokitoh, *J. Organomet. Chem.*, 2007, **692**, 44–54.

19 H. Lee, S.-O. Hauber, D. Vinduš and M. Niemeyer, *Inorg. Chem.*, 2008, **47**, 4401–4412.

20 G. Jin, C. Jones, P. C. Junk, K.-A. Lippert, R. P. Rose and A. Stasch, *New J. Chem.*, 2008, **33**, 64–75.

21 A. M. Willcocks, T. P. Robinson, C. Roche, T. Pugh, S. P. Richards, A. J. Kingsley, J. P. Lowe and A. L. Johnson, *Inorg. Chem.*, 2011, **51**, 246–257.

22 A. K. Maity, S. Fortier, L. Griego and A. J. Metta-Magaña, *Inorg. Chem.*, 2014, **53**, 8155–8164.

23 M. Magre, M. Szewczyk and M. Rueping, *Chem. Rev.*, 2022, **122**, 8261–8312.

24 C. Schmitz, H.-W. Schmidt and M. Thelakkat, *Chem. Mater.*, 2000, **12**, 3012–3019.

25 O. Back, C. Förster, T. Basché and K. Heinze, *Chem. – Eur. J.*, 2019, **25**, 6542–6552.

26 T. J. Feuerstein, B. Goswami, P. Rauthe, R. Köppe, S. Lebedkin, M. M. Kappes and P. W. Roesky, *Chem. Sci.*, 2019, **10**, 4742–4749.

27 P. Pinter, C. M. Schüßlbauer, F. A. Watt, N. Dickmann, R. Herbst-Irmer, B. Morgenstern, A. Grünwald, T. Ullrich, M. Zimmer, S. Hohloch, D. M. Guldi and D. Munz, *Chem. Sci.*, 2021, **12**, 7401–7410.

28 M. Kaiser, M. P. Müller, F. Krätschmer, M. Rutschmann and A. Hinz, *Inorg. Chem. Front.*, 2023, **10**, 2987–2994.

29 R. Yoshii, A. Hirose, K. Tanaka and Y. Chujo, *Chem. – Eur. J.*, 2014, **20**, 8320–8324.

30 R. Yoshii, A. Hirose, K. Tanaka and Y. Chujo, *J. Am. Chem. Soc.*, 2014, **136**, 18131–18139.

31 M. Yamaguchi, S. Ito, A. Hirose, K. Tanaka and Y. Chujo, *J. Mater. Chem. C*, 2016, **4**, 5314–5319.

32 S. Ito, A. Hirose, M. Yamaguchi, K. Tanaka and Y. Chujo, *J. Mater. Chem. C*, 2016, **4**, 5564–5571.

33 M. Yamaguchi, S. Ito, A. Hirose, K. Tanaka and Y. Chujo, *Mater. Chem. Front.*, 2017, **1**, 1573–1579.

34 S. Ito, K. Tanaka and Y. Chujo, *Inorganics*, 2019, **7**, 100.

35 S. Ito, M. Yaegashi, K. Tanaka and Y. Chujo, *Chem. – Eur. J.*, 2021, **27**, 9302–9312.

36 Y. Aoyama, Y. Sakai, S. Ito and K. Tanaka, *Chem. – Eur. J.*, 2023, **29**, e202300654.

37 S. Ito, M. Hashizume, H. Taka, H. Kita, K. Tanaka and Y. Chujo, *Mater. Chem. Front.*, 2023, **7**, 4971–4983.

38 S. Ito, K. Tanaka and Y. Chujo, *Dalton Trans.*, 2024, **53**, 14858–14865.

39 S. Ito, T. Hosokai, K. Tanaka and Y. Chujo, *Commun. Chem.*, 2024, **7**, 202.

40 M. Arrowsmith, M. R. Crimmin, M. S. Hill and G. Kociok-Köhn, *Dalton Trans.*, 2013, **42**, 9720–9726.

41 H. Chen, R. A. Bartlett, H. V. R. Dias, M. M. Olmstead and P. P. Power, *Inorg. Chem.*, 1991, **30**, 2487–2494.